A Framework for 3D Analysis of Facial Morphology in Fetal Alcohol Syndrome

Jing Wan[1,2,4], Li Shen[1,2,⋆], Shiaofen Fang[1], Jason McLaughlin[1], Ilona Autti-Rämö[5], Åse Fagerlund[6], Edward Riley[7], H. Eugene Hoyme[8], Elizabeth S. Moore[9], Tatiana Foroud[3,⋆], and Collaborative Initiative on Fetal Alcohol Spectrum Disorders (CIFASD)

[1]Dept. of Computer and Info. Science, Purdue University, Indianapolis, IN, USA
[2]Dept. of Radiology and Imaging Sciences, [3]Dept. of Medical and Molecular Genetics, Indiana University School of Medicine, Indianapolis, IN, USA
[4]Jiangxi University of Finance and Economics, Jiangxi, China
[5]Dept. of Child Neurology, HUCH Hospital for Children & Adolescents, Findland
[6]Folkhälsan Research Center, Helsinki, Finland
[7]Department of Psychology, San Diego State University, CA, USA
[8] Sanford School of Medicine, University of South Dakota, Vermillion, SD, USA
[9]St. Vincent Women's Hospital, Indianapolis, IN, USA

Abstract. Surface-based morphometry (SBM) is widely used in biomedical imaging and other domains to localize shape changes related to different conditions. This paper presents a computational framework that integrates a set of effective surface registration and analysis methods to form a unified SBM processing pipeline. Surface registration includes two parts: surface alignment in the object space by employing the iterative closest point (ICP) method, and surface alignment in the parameter space by using conformal mapping and landmark-based thin-plate spline methods. Statistical group analysis of registered surface data is then conducted by surface-based general linear model and random field theory addressing multiple testing issues. The effectiveness of the proposed framework is demonstrated by applying it to a fetal alcohol syndrome (FAS) study for identifying facial dysmorphology in FAS patients.

1 Introduction

The adverse effects of alcohol on the developing fetus fall along a continuum. The collection of these disorders is known as fetal alcohol spectrum disorders (FASD). Fetal alcohol syndrome (FAS), considered as a more severe subset of FASD, can be defined by recognizable facial dysmorphology, growth deficits, and behavioral problems [6]. Individuals diagnosed with FAS present a pattern of minor facial anomalies including short palpebral fissures, flat nasal bridge, smooth philtrum, thin upper lip, and flat mid-face [12]. The ongoing clinical

⋆ Correspondence to L. Shen (shenli@iupui.edu) or T. Foroud (tforoud@iupui.edu).
Supported in part by NIAAA U01 AA014809 and NIBIB R03 EB008674. The original publication is available at www.springerlink.com.

challenge is to expand the recognizable facial features so more individuals with prenatal alcohol exposure that do not exhibit the classic facial phenotype can be identified, allowing for early interventions.

Craniofacial anthropometry has been used to accurately identify individuals with FAS [13]. However, anthropometric assessments can be time consuming and usually require an experienced anthropometrist to obtain the measurements. So there is a need for newer techniques, which in combination with a clinician's assessment, would provide rapid and accurate pre-screening and early diagnosis of children with a FASD [6]. Three-dimensional (3D) surface-based morphometry offers the opportunity to solve the problem.

Surface-based morphometry (SBM), widely used in biomedical imaging to study various structures of interest, is used to identify morphometric abnormalities associated with a particular condition, assisting with diagnosis and treatment. Many studies [3, 9] of facial morphology focus on the delineation of characteristic features or building computational models of face-shape variation. Hammond et al. [9] proposed a dense surface model of the huaman face. They used 3D thin-plate spline (TPS) to align the landmarks of each face, employed iterative closest point (ICP) method to build correspondence by taking the closest point on each surface from each vertex on a base mesh, and then applied the inverse of the TPS warp to map each surface back to its original location. The base mesh was chosen as an individual from the data and thus not a regular mesh. Using such a base mesh to sample other meshes may not be ideal for SBM which typically works on a uniformly sampled surface manifold. In addition, since 3D TPS has no analytical inverse, the error introduced by approximating the TPS inverse and its computational complexity are unclear. Wang et al. [21] proposed a non-rigid 3D motion tracking algorithm using harmonic maps with added feature correspondence constraints to build dense one-to-one inter-frame correspondences. This method may not be applicable to data sets where only geometric information is available or surface correspondence cannot be implicated by texture information.

Here we propose a novel computational framework that performs SBM on 3D facial imaging data and demonstrate its effectiveness via an FAS application. We are given two groups of 3D facial surfaces represented by triangular meshes. Each mesh is assumed to have a disk topology and does not contain any hole. A set of landmarks are available on each mesh to pre-define a coarse correspondence between surfaces. Our goal is to localize morphological changes related to the group condition (i.e., FAS versus controls). Our SBM framework includes three key components: (1) Surface alignment in the object space is achieved by employing the ICP algorithm. (2) Surface registration in the parameter space is obtained by using conformal mapping and landmark-based 2D TPS methods. (3) Statistical group analysis of registered surface data is conducted directly on the surface manifold to avoid distortion introduced by surface flattening, and a surface-based general linear model with random field theory is used to achieve this goal and address multiple testing issues.

Our approach sacrifices full automation by using landmarks in exchange for more robustness and higher accuracy to surface registration, allowing users to define critical locations where surface correspondence should be established. Instead of directly working in 3D domain like [9], our approach establishes the surface correspondence via a 2D parametric domain, making the entire processing pipeline simple, efficient, and easy to implement and interpret. While this pipeline is demonstrated in an FAS study, it is a general framework and could be applied to other 3D surface objects with disk-like topology and landmarks.

2 Materials and Methods

2.1 Data Set

The data set used in this study included 44 (18 males and 26 females, age 13.0 ± 3.6) FAS and 52 (20 males and 32 females, age 13.9 ± 3.6) healthy control (HCL) participants from Helsinki, Finland. The participants or their legal guardians provided written informed consents. Each participant was examined and classified as FAS, no FAS, or deferred according to a standardized assessment [11]. Preliminary diagnosis was determined on the basis of facial structural features and growth deficiency consistent with the revised Institute of Medicine criteria [10]. The final diagnoses were considered with alcohol exposure data which were collected through a standard questionnaire consisting of four questions in the interview or from a review of available study data. This study only included the individuals determined as FAS with prenatal alcohol exposure and the ones designated as no FAS without prenatal alcohol exposure.

A standard scheme was utilized to collect 3D facial images using Minolta Vivid 910 laser scanners. Each participant was seated approximately 660 mm from the scanner and six scans were taken as: two frontal, two 45 degree to the right of the frontal axis, and two 45 degree to the left of the frontal axis. These three directions of scans ensured the entire facial area was covered. A stitching processing using a commercially available software package, Rapidform 2004, was applied to merge the scans of the three views into one single 3D surface image [6]. 33 landmarks (Figure 1) were then manually defined by a trained technician. The landmarks were prominent and easily identifiable points on each face (e.g. the corners of the eyes). They provide meaningful constraints for regions of interest in facial dysmorphology to guide the registration procedure.

2.2 Surface Registration

We first register all the surfaces in the object space. The iterative closest point (ICP) algorithm [1] is used to register each surface to a template surface, which is pre-selected as an HCL surface. This rigid transformation normalizes the orientation and location of each surface. After that, surface correspondence is established via 2D parameterization, where conformal mapping and 2D thin-plate

spline (TPS) [2] are employed. Our goal is to achieve a smoothing mapping between any surface and the 2D parameter domain, and assign the same landmark of different models with the same location in the parameter space.

We first describe how conform mapping is implemented. To perform statistical shape analysis on 3D facial surfaces, we need to establish a meaningful correspondence between them. One way to achieve the goal is to map these facial surfaces into a standard space while preserving geometric information on the original structures as much as possible [7, 8]. So this becomes a surface parameterization problem.

Surface parameterization, defined as one-to-one mapping from a surface into another parameter domain, can always introduce distortion in either angles or areas [7]. A good mapping is the one which minimizes the distortions to some extent. To achieve this goal, conformal mapping is one way to minimize the angular distortion [8]. Riemann theorem states that conformal mapping of a smooth surface into a plane exists for any simply-connected plane domain [4]. Since meshes of a smooth surface can be viewed as approximations of the surface, it is possible to map them to a plane with very little angular distortion [15].

Before describing the comformal mapping algorithm used in our framework, we first introduce some basic concepts. Suppose a surface $M_1 \subset \mathbb{R}^3$ has the parametric representation $\mathbf{x}(u^1, u^2) = (x_1(u^1, u^2), x_2(u^1, u^2), x_3(u^1, u^2))$ for points (u^1, u^2) in some domain in $\mathbb{R}^2$. The first fundamental form of M_1 is

$$ds_1^2 = \sum_{ij} g_{ij} du^i du^j \quad \text{where} \quad g_{ij} = \frac{\partial \mathbf{x}}{\partial u^i} \cdot \frac{\partial \mathbf{x}}{\partial u^j} \ (i, j = 1, 2) \tag{1}$$

Another plane $M_2 \subset \mathbb{R}^2$ is similarly represented by $\widetilde{\mathbf{x}}(\tilde{u}^1, \tilde{u}^2)$. Define a mapping $f : M_1 \mapsto M_2$ between two surfaces. If f is a conformal mapping, then there is some scalar function $\eta \neq 0$, such that $ds_1^2 = \eta(\tilde{u}^1, \tilde{u}^2)((d\tilde{u}^1)^2 + (d\tilde{u}^2)^2)$. As shown in [7], two Laplace's equations are obtained as

$$\triangle_s \tilde{u}^1 = 0, \ \triangle_s \tilde{u}^2 = 0 \tag{2}$$

$\triangle_s$ is the Laplace-Beltrami operator, which can be written as $\triangle_s = \mathrm{div}_s \mathrm{grad}_s$. To find the solution to Equation (2), the conformal mapping f can be viewed as minimizing the Dirichlet energy:

$$E_0(f) = \frac{1}{2} \int_s \|\mathrm{grad}_s f\|^2 \tag{3}$$

To compute f, Eck et al. [5] proposed an approach, called discrete harmonic map, which extends the graph embedding method of Tutte [19]. In their method, the boundary vertices of the meshes are first mapped to the boundary of the unit disk. Then the positions of the remaining vertices can be computed by solving equations:

$$L\tilde{u}^1 = 0, \qquad L\tilde{u}^2 = 0 \tag{4}$$

$$L_{ij} = \begin{cases} -\sum_{k \neq i} L_{ik}, & i = j \\ w_{ij}, & (i, j) \in E \\ 0, & \text{otherwise} \end{cases} \tag{5}$$

$$w_{ij} = \cot \alpha_{ij} + \cot \beta_{ij}, \tag{6}$$

where α_{ij} and β_{ij} are the opposite angles in the two triangles sharing an edge (i, j) [15].

This study employs Eck's method to perform conformal mapping from 3D facial meshes to 2D meshes in the unit disk. A public matlab toolbox, Toolbox Graph [14], is used to implement the algorithm. Here we perform conformal mapping to map each vertex of a 3D mesh to the corresponding 2D position in a unit disk with fixed boundary. Suppose an individual is represented as a set of vertices (Xa, Ya, Za). After applying conformal mapping Φ, which is bijective, each individual gets new coordinates $(\Phi(Xa), \Phi(Ya))$ in the 2D disk domain. As an example, let the height (i.e., Z value of each vertex in the original model) be the geometric information of our interest, and thus the mapped individual can be represented as $(\Phi(Xa), \Phi(Ya), Za)$. Of note, other surface features (e.g., x, y coordinates, curvature, etc.) can be studied in the same way. For simplicity, we explain our method here by focusing on z coordinates only.

After applying conformal mapping to all the subjects in the data set, we pick a healthy individual as the template and then register all the subjects to the template using landmark based thin-plate splines (TPS) warp Ψ [2] in the 2D domain. Now the landmarks of each individual are exactly aligned to those of the template. The remaining parts of the individuals are interpolated according to the movement of their landmarks. An individual can then be represented as $(\Psi(\Phi(Xa)), \Psi(\Phi(Ya)), Za)$, where Ψ denotes the TPS registration function.

Since each individual mesh has different number of vertices and triangles, we need to resample them using a regular mesh grid defined in the disk. After resampling, all the individuals in the data set have the same mesh topology and can be compared with each other. Z-coordinates (i.e., heights) of the re-sampled points can be obtained by using cubic interpolation for each individual, and are used to extract surface signals in subsequent analyses.

2.3 Statistical Shape Analysis

After surface registration, all facial surfaces are aligned to the same reference system. This facilitates the subsequent analysis on the facial surfaces, including extracting surface signals and performing statistical inference on the surface manifold using general linear model (GLM) [17, 20]. We use X_t to denote the atlas, which is computed as an average of all registered healthy controls (HCLs). For an individual surface X, we use its deformation field $\delta(X) = X - X_t$ as surface signals to describe the shape based on the atlas X_t. In this study, we examine two types of surface shape signals: (1) deformation scalar along z-axis direction and (2) mean curvature of each vertex.

Remember our goal is to detect significant shape changes on facial surfaces between HCL group and FAS group. We consider the following GLM

$$y = X\Psi + Z\Phi + \epsilon \tag{7}$$

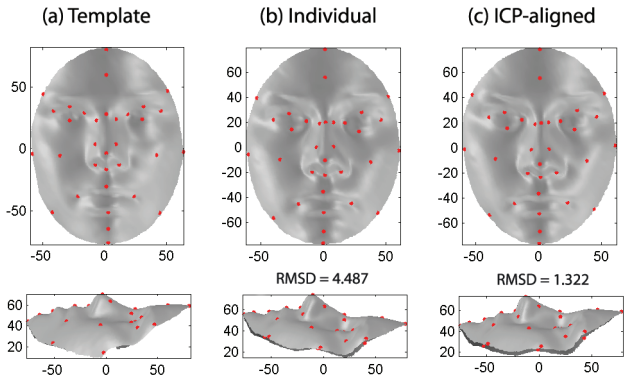

Fig. 1. Registration in the object space by aligning an individual to the template using ICP: (1) template, (2) individual, and (3) ICP-aligned individual.

where the dependent variable y is our surface signal; $X = (x_1, \cdots, x_p)$ are the variables of interest such as Group; $Z = (z_1, \cdots, z_k)$ are the variables whose effects we want to exclude, such as Age and Gender; and $\Psi = (\psi_1, \cdots, \psi_p)^T$ and $\Phi = (\phi_1, \cdots, \phi_k)^T$ are the coefficients; and ϵ is the error term. The goal is to test if X is significant (i.e. $\Psi \neq 0$) for $y \in \partial\Omega$, where $\partial\Omega$ indicates the surface manifold. We use SurfStat to test our GLMs. SurfStat is a Matlab toolbox for statistical analysis of univariate and multivariate surface and volumetric data using linear mixed effects models and random field theory (RFT) [22]. Using SurfStat notation (coefficients excluded in the equation), we examine the following two models, where dependent variables (i.e. y in Eq.(7)) are our surface signals defined above, and RFT is used for multiple comparison correction.

Model	Description
M1 = 1 + Status	Diagnosis effect on surface signals
M2 = 1 + Status + Age + Gender	Diagnosis effect on surface signals with controlling Age and Gender effect

3 Experimental Results

3.1 Surface Registration

Figure 1 shows an example of registration result in the object space by aligning an individual to the template using ICP, which normalizes the orientation and location of the initial configuration. The root mean square distance (RMSD) between the individual and the template before ICP registration is 4.487 and it is reduced to 1.322 after ICP registration.

Figure 2 shows a sample registration procedure in the parameter space by aligning an individual's conformal map (d) to the template conformal map (c) using TPS. While landmarks are aligned perfectly between the individual and the template, a smooth mapping from the individual to the template is obtained

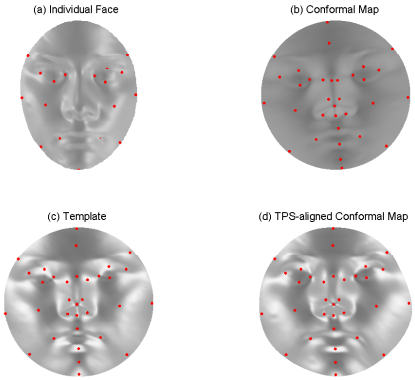

Fig. 2. Registration in the parameter space by aligning an individual's conformal map to the template conformal map using TPS: (1) individual face, (2) individual conformal map, (3) template conformal map, and (4) TPS-aligned individual conformal map.

for establishing the surface correspondence. To quantify the registration quality, we consider two factors: (1) the area distort cost (ADC) (defined in [16]) from the object surface to the parameter domain (i.e., 2D disk), and (2) RMSD between landmarks of the individual and the template in the parameter domain. Our goal is to achieve RMSD=0 while controlling the area distortion ADC. If we just use conformal mapping, we have ADC of 1.1508 ± 0.0231 (mean±std) and RMSD of 0.6841 ± 0.1124 for all the subjects in our data. If we combine conformal mapping with TPS, we have ADC of 1.3723 ± 0.0987 and RMSD of 0 ± 0. In this case, although our ADC gets slightly increased, RMSD=0 guarantees that all the landmarks are perfectly aligned across all the subjects.

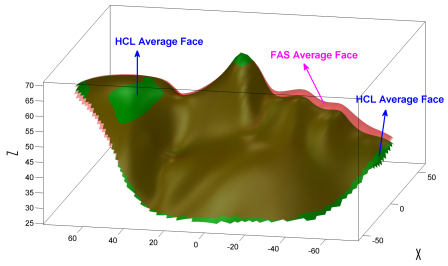

Fig. 3. HCL average face and FAS average face: HCL average face is used as the atlas for extracting surface signals.

Figure 3 shows the average of all the HCL faces and the average of all the FAS faces. The HCL average face is used as the atlas for extracting surface signals.

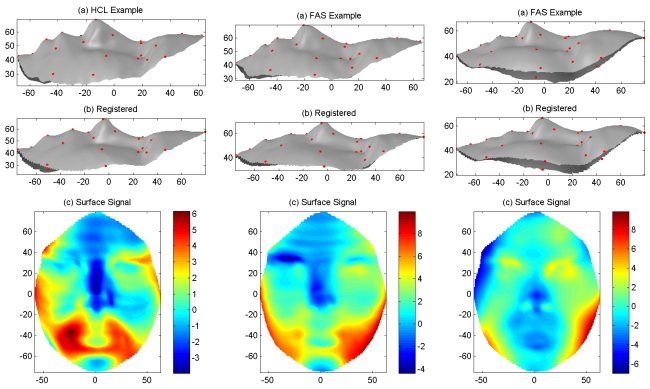

Fig. 4. One HCL and two FAS examples of surface registration and signal extraction results: (a) original surface, (b) registered surface, and (c) surface signals. Note that the x, y coordinates of landmarks after registration are consistent across subjects (see (b)). For each participant, the landmark z values (i.e., heights) stay the same before and after registration (see (a-b)).

Figure 4 shows the surface registration and signal extraction results for one HCL and two FAS examples. The three facial surfaces after being aligned in object space are shown in Figure 4(a) and their registered surfaces after conformal mapping and TPS are shown in (b). Note that the x, y coordinates of landmarks after registration in parameter domain are consistent across subjects (see (b)). For each participant, the landmark z values (i.e., heights) stay the same before and after registration (see (a-b)). (c) shows the surface signals we extract from the three surfaces. The surface signals visualized here are deformation scalar along z-axis direction (i.e. height). Red color represents positive surface signal value while blue color denotes negative surface signal value.

3.2 Statistical Shape Analysis

As mentioned in Section 2.3, we examine diagnosis effect on surface signals between HCL and FAS, with and without involving age and gender as covariates in Model M_2 and Model M_1, respectively. Since the results of M_1 and M_2 are very similar, only M_2 results are shown in Figure 5: (a,c) the maps of the t statistics, (b,d) the maps of corrected P values for peak and clusters (only regions with $p \leq 0.01$ are color-mapped). Let us first look at the height results (a,b). As described earlier, the signal at each surface location is defined as the deformation from the atlas to an individual along z-axis direction. So the signals take either positive values for outward deformations or negative values for inward deformations. As the contrast of M_2 is defined as "FAS−HCL", the colorful T maps in (a) can be explained as follows: the shape of an FAS face tends to be contractive in the red regions and expansive in the blue regions compared to that of an HCL face. All the significant regions in (b) correspond to the red regions in (a), indi-

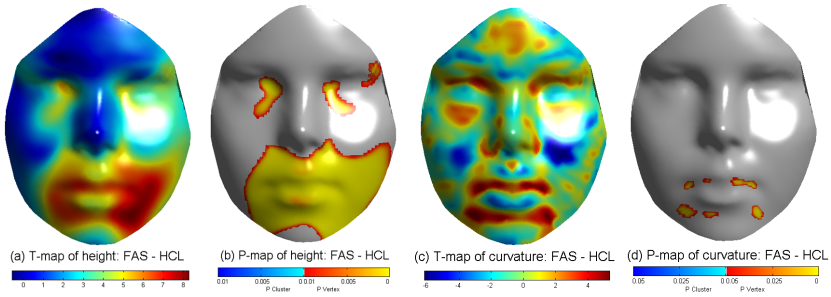

Fig. 5. Diagnosis effect (i.e., FAS-HCL) on surface signals (heights in (a,b), curvatures in (c,d)) while controlling for Age and Gender. (a,c) show the maps of the t statistics. (b,c) show the maps of corrected P values for peak and clusters with $p \leq 0.01$.

cating FAS faces are expansive in those regions compared to HCL faces. When P threshold is set to 0.01, the significant regions cover the corner of two eyes, lips, and philtrum. These results are in accordance with previously known facial features for FAS diagnosis (e.g., short palpebral fissures, upper lip and smooth philtrum [10, 18]). As to the curvature results (c,d), while few significant areas are identified in P-map (d), the T-map (c) shows a very interesting red region in the philtrum. Since curvatures in a philtrum region usually take negative values indicating concave, red color of that region in (c) denotes larger curvature values in FAS than in HCL and consequently smoother philtrum in FAS. This matches the existing findings.

4 Conclusions

In this paper, we presented a novel computational framework for surface based morphometry (SBM). It integrated a set of effective surface registration and analysis methods to form a unified SBM processing pipeline. Three parts were included in this pipeline: (1) surface alignment in the object space by performing the iterative closest point algorithm, (2) surface registration in the parameter space by employing conformal mapping and landmark-based thin-plate spline methods, and (3) statistical group analysis on registered facial surfaces by using general linear model with random field theory. This framework was applied to 3D analysis of facial morphology in fetal alcohol syndrome (FAS). The goal was to identify regional facial changes of the FAS group compared to healthy controls using 3D facial imaging data. The results identified facial dysmorphology patterns in FAS that were consistent with prior findings. This demonstrated the effectiveness of our framework. The framework is relatively simple and efficient. It can be applied to other applications dealing with similar data and derive results that are easy to interpret. One interesting future direction could be to examine additional surface signals such as tensors and displacement vectors. Another direction would be to apply this technique to individuals with known alcohol exposure that do not exhibit the classic FAS face.

References

1. Besl, P.J., McKay, N.D.: A method for registration of 3-d shapes. IEEE Trans. on Pattern Analysis and Machine Intelligence 14(2), 239–256 (1992)
2. Bookstein, F.L.: Shape and the information in medical images: a decade of the morphometric synthesis. Comput. Vis. Image Underst. 66(2), 97–118 (1997)
3. Bronstein, A.M., Bronstein, M.M., Kimmel, R.: Calculus of nonrigid surfaces for geometry and texture manipulation. IEEE Trans. on Visualization and Computer Graphics 13(5), 902–913 (2007)
4. do Carmo, M.P.: Differential geometry of curves and surfaces. Prentice Hall (1976)
5. Eck, M., DeRose, T.D., Duchamp, T., et al.: Multiresolution analysis of arbitrary meshes. In: Proc. of ACM SIGGRAPH '95. pp. 173–182 (1995)
6. Fang, S., McLaughlin, J., et al.: Automated diagnosis of fetal alcohol syndrome using 3D facial image analysis. Orthodontics & Craniofacial Res. pp. 162–171 (2008)
7. Floater, M.S., Hormann, K.: Surface parameterization: a tutorial and survey. In: Advances in Multiresolution for Geometric Modelling. pp. 157–186. Springer (2005)
8. Gu, X., Wang, Y., et al.: Genus zero surface conformal mapping and its application to brain surface mapping. IEEE Trans. on Medical Imaging 23(8), 949–958 (2004)
9. Hammond, P., Hutton, T.J., Allanson, J.E., et al.: 3D analysis of facial morphology. American Journal of Medical Genetics 126A, 339–348 (2004)
10. Hoyme, H., May, P., Kalberg, W., et al: A practical clinical approach to diagnosis of fetal alcohol spectrum disorders: Clarification of the 1996 institute of medicine criteria. Pediatrics pp. 39–47 (2005)
11. Jones, K.L., Robinson, L.K., Bakhireva, L.N., et al: Accuracy of the diagnosis of physical features of fetal alcohol syndrome by pediatricians after specialized training. Pediatrics 118, 1734–1738 (2006)
12. Jones, K.L., Smith, D.W.: Recognition of the fetal alcohol syndrome in early infancy. Lancet 2, 999–1001 (1973)
13. Moore, E.S., Ward, R.E., Wetherill, L.F., et al.: Unique facial features distinguish fetal alcohol syndrome patients and controls in diverse ethnic populations. Alcoholism: Clinical and Experimental Research 31, 1707–1713 (2007)
14. Peyre, G.: Toobox_Graph:http://www.ceremade.dauphine.fr/∼peyre/matlab/graph/content.html
15. Sheffer, A., Praun, E., Rose, K.: Mesh parameterization methods and their applications. Found. Trends. Comput. Graph. Vis. 2(2), 105–171 (2006)
16. Shen, L., Farid, H., McPeek, M.A.: Modeling 3-dimensional morphological structures using spherical harmonics. Evolution 63(4), 1003–1016 (2009)
17. Shen, L., Saykin, A., Chung, M.K., et al.: Morphometric analysis of hippocampal shape in mild cognitive impairment: an imaging genetics study. In: IEEE 7th Int. Sym. on Bioinformatics and BioEngineering. pp. 211–217. Boston, MA (2007)
18. Stoler, J.M., Holmes, L.B.: Recognition of facial features of fetal alcohol syndrome in the newborn. American Journal of Medical Genetics Part C 127(1), 21–27 (2004)
19. Tutte, W.T.: How to draw a graph. London Mathematical Soc. 13, 743–768 (1963)
20. Wan, J., Shen, L., Sheehan, K.E., et al: Shape analysis of thalamic atrophy in multiple sclerosis. In: MIAMS. pp. 93–104. Imperial College London, UK (2009)
21. Wang, Y., Gupta, M., et al.: High resolution tracking of non-rigid 3d motion of densely sampled data using harmonic maps. Int. Conf. on Computer Vision (2005)
22. Worsley, K.J., Andermann, M., Koulis, M., et al.: Detecting changes in non-isotropic images. Human Brain Mapping 8, 98–101 (1999)